Neal Michelutti (ORCID ID: 0000-0002-5857-4811)
Kathryn E. Hargan (ORCID ID: 0000-0002-2232-3711)
John P. Smol (ORCID ID: 0000-0002-2499-6696)
Jules M. Blais (ORCID ID: 0000-0002-7188-3598)

Using stable water isotope composition ($\delta^{18}O$ and $\delta^{2}H$) to track the interannual responses of Arctic and tropical Andean water bodies to rising air temperatures

Neal Michelutti[1,2,*], Kathryn E. Hargan[2,3,4], Linda E. Kimpe[3], John P. Smol[1], Jules M. Blais[3]

[1]Paleoecological Environmental Assessment and Research Lab (PEARL), Department of Biology, Queen's University, Kingston, Ontario K7L 3N6, Canada.

[2]N.M. and K.E.H. contributed equally to this work

[3]Department of Biology, University of Ottawa, Ottawa, ON Canada K1N 6N5, Canada

[4]Current address: Department of Biology, Memorial University of Newfoundland, 232 Elizabeth Ave., St. John's, NL

*Correspondence to: Neal Michelutti (nm37@queensu.ca)

Key Points

- $\delta^{18}O$ and $\delta^{2}H$ data from Arctic waterbodies showed evaporative loss from small ponds, whereas large, ice-covered lakes were less prone to evaporation.
- Stable water isotopes from Andean lakes showed that temperature-driven evaporative water loss was offset by abundant precipitation.
- The Arctic and Andean data indicate the importance of future precipitation trends for maintaining these ecologically and societally important waterbodies.

Abstract

Lakes in the Arctic and tropical Andes are experiencing some of the largest temperature increases on the planet with coeval marked limnological changes, but little data exist on water balance parameters from these regions. Here, we present a unique data set of water stable isotope composition ($\delta^{18}O$ and $\delta^{2}H$) from a suite of 49 waterbodies in the Canadian Arctic (Resolute Bay, Cornwallis Island, and Cape Herschel, Ellesmere Island) and the tropical Andes (Cajas National Park, Ecuador) spanning various years from 2009 to 2016. We show that an increase in air temperature over the study period resulted in evaporative enrichment of water isotopes in most Arctic sites highlighting the significance of evaporative losses to small Arctic ponds during the prolonged ice-free summers now experienced in this part of the world. Exceptions include some Arctic waterbodies that received abundant snowmelt and large, ice-covered lakes less prone to evaporation. Data from the Andean lakes indicated evaporative effects were minimal due to abundant precipitation. These data, in combination with limnological records and paleolimnological research from each region, provide a holistic view on how freshwater ecosystems are responding to recent warming in climatically sensitive Arctic and Andean environments.

Plain Language Summary

Arctic and alpine ecosystems have recorded amongst the largest temperature increases on the planet in recent decades and lakes in these regions have already changed in unprecedented ways. Of particular concern is the temperature-driven increases in evaporation, which may affect the permanency of these waterbodies. Here, we track trends in evaporative loss from a suite of waterbodies in the Canadian High Arctic and Ecuadorian Andes. We show that the recent temperature increases in the Canadian Arctic have resulted in discernible signs of evaporation, especially in small, shallow ponds. In the Andes, the effect of rising temperature on evaporative loss is offset by abundant precipitation during the rainy season. Our data show the importance of future trends in precipitation to maintain and recharge these waterbodies, which are critical to regional biodiversity and an important water resource for local populations.

Key words: stable isotopes, oxygen, hydrogen, freshwater, climate

1. Introduction

Over the past three decades, Arctic and Andean regions have warmed at a rate approximately twice the global average (Diaz et al., 2014; Larsen et al., 2014). Lakes in these environments have responded to recent warming in a variety of ways including changes in water quality variables (Roberts et al., 2017; Smol and Douglas, 2007a, b), alterations to thermal structure (Michelutti et al., 2016; Saros et al., 2016), and regime shifts in aquatic biodiversity and species abundances (Michelutti et al., 2015; Smol et al., 2005). Stable oxygen and hydrogen isotopes of water respond sensitively to hydroclimate variability and can provide information on hydrological variables, such as evaporation, which is not detected by other limnological monitoring methods. For example, stable isotope composition of oxygen ($\delta^{18}O$) and hydrogen ($\delta^{2}H$) in surface waters have been used to track changes in runoff, outflow, residence times and evaporation in Arctic and Andean regions (MacDonald et al., 2017; 2021; Cluett and Thomas, 2020; Esquivel-Hernandez et al., 2018; Gibson and Reid, 2014).

The primary input water of a lake is typically from precipitation. Isotope variations in precipitation are generally characterized by strong linear correlations between $\delta^{18}O$ and $\delta^{2}H$ that reflect mass-dependent partitioning of the water isotopes in the hydrological cycle. This coupling is exemplified by the Global Meteoric Water Line (GMWL; Craig, 1961), which closely approximates the observed relation between $\delta^{2}H$ and $\delta^{18}O$ in mean annual amount-weighted precipitation world-wide. The isotopic composition of precipitation collected from a single site or region, known as the Local Meteoric Water Line (LMWL), can vary from the GMWL largely because of variability in humidity during primary evaporation of water vapour from the ocean and the temperature of condensation of the precipitation (Benjamin et al., 2004).

In a plot of $\delta^{2}H$ - $\delta^{18}O$, the intersection of regional local evaporation lines (LELs), calculated by linear regressions of $\delta^{18}O$ and $\delta^{2}H$ from several neighboring waterbodies, with the LMWL can approximate the isotopic composition of source water, while displacement of surface waters along the LEL provides an indication of water balance variables, including evaporation (Edwards et al., 2004). Deuterium excess (d-excess = $\delta^{2}H - 8\delta^{18}O$) is a second-order stable isotope parameter that informs about the source region of precipitation and moisture changes during transport (Bershaw, 2018). In surface waters, d-excess values generally vary inversely with evaporation (Bowen et al., 2019; Wen et al., 2016).

Lakes in the Arctic and Andes are exposed to markedly different environmental conditions. For example, Arctic regions exhibit extreme seasonal variation with distinct (and often short) open-water seasons, whereas tropical Andean regions are characterized by minimal seasonality with more pronounced diel variations, perennially ice-free conditions, and near constant evaporation rates throughout the year. Yet, tropical Andean lakes share many functional similarities with their Arctic counterparts including generally cool water temperatures, oligotrophic conditions, and simple food webs. Moreover, physical properties of Arctic and Andean lakes are primarily governed by temperature and wind, and thus climate variability may subject them to similar changes. In fact, over the last few decades, Arctic and equatorial Andean lakes both recorded enhanced and prolonged thermal stratification measured via direct lake water temperatures (Michelutti et al., 2016) and inferred through similar regime shifts in phytoplankton communities (Griffiths et al., 2017; Michelutti et al., 2015; Rühland et al., 2015). Given the parallel responses in thermal structure and diatom assemblage shifts recorded in our Arctic and Andean study lakes, stable isotopes of water may provide information on similarities/differences with respect to water balance parameters (e.g., evaporation).

Here, we present water isotope data ($\delta^{18}O$ and $\delta^{2}H$) from a suite of water bodies in both the Arctic and Andes, spanning various years from 2009 to 2016, to better understand broad patterns of water balance within and among the study regions, where water supply is dominated by precipitation. The Arctic sites are in Nunavut (Canada) and include Resolute Bay on Cornwallis Island (n=11) and Cape Herschel on Ellesmere Island (n=29). The Andean lakes (n=9) are in the southern sierra of Ecuador, near the city of Cuenca (Fig. 1). The three study regions contain a network of lakes and ponds that form a semi-continuous monitoring program with past research focusing on water chemistry, thermal mixing regimes, and paleolimnological analyses (Douglas and Smol, 1993; Douglas et al., 1994; Griffiths et al., 2017; Labaj et al., 2018; Michelutti et al., 2016, 2015). We examined lake water isotope compositions from each study region to address three central questions. First, how do lakewater $\delta^{18}O$ and $\delta^{2}H$ values at each study site vary among years and can any changes be related to temperature records from nearby meteorological stations? Second, in the Arctic study regions, are there differential responses in $\delta^{18}O$ and $\delta^{2}H$ values among years between large lakes that retain ice cover well into the summer months versus shallow ponds that melt earlier in the growing season? Third, what are the similarities/differences between Arctic and Andean regions with respect to any changes in $\delta^{18}O$ and $\delta^{2}H$ values and their relationship to temperature variability? These data contribute to a growing limnological database for Arctic and Andean regions and provide baseline data to assess future changes in regional water cycles.

2. Materials and Methods

2.1 Regional settings and sample collection

Resolute Bay, Cornwallis Island, Nunavut – Resolute Bay (Qausuittuq) is the only permanent settlement on Cornwallis Island (Fig. 1). The island is of relatively low relief (max elevation = 411 m asl) and contains no ice-caps or glaciers. Climate normals (1971-2000) from the Resolute Bay weather station (available from http://climate.weather.gc.ca/), centrally situated from the study sites, show a mean annual temperature of –16.4°C, with July being the warmest month at +4.3 °C and February the coldest at -33.1°C. Since the start of meteorological records in 1948, air temperatures have increased steadily until present-day (Environment Canada, 2016; Stewart et al., 2014). The region is a polar desert, receiving only 150 mm of precipitation annually, with approximately two-thirds occurring as snow (Environment Canada, 2016).

Eleven lakes and ponds were sampled from the Resolute Bay region during July of 2009, 2011, and 2014 (Table 1). Although not all sites were sampled each year, sites were re-sampled at least two of the three years. Mean dates of June 17 for thaw and August 26 for freeze-back leave slightly over two months of above freezing conditions (Woo and Young, 2003). Most of the Resolute Bay study sites are shallow ponds (< 2 m depth) and thus can reach relatively warm temperatures (5 – 10°C); however, during extremely cool years the larger study lakes (e.g., Char Lake) may retain partial ice cover for the entire summer (Schindler et al., 1974).

Cape Herschel and Pim Island, Ellesmere Island, Nunavut – Twenty-five study sites were sampled on Cape Herschel, which is located on east-central Ellesmere Island, during July of 2009 and 2011 (Table 1). Four additional sites were sampled on nearby Pim Island (~10 km to the northeast), which is a small island (~86 km^2) with a maximum elevation of 550 masl (Fig. 1). The Cape Herschel sites have been sampled at irregular intervals since 1983, as part of a long-term limnological monitoring program (Douglas and Smol, 1993; Smol and Douglas, 2007a, b; Griffiths et al., 2017). Although glaciers are nearby, none of them drain into the study sites.

Climate normals (1981-2010) from the nearest meteorological station to Cape Herschel (Eureka A; ~280 km west and ~1°N) show a mean annual temperature of -19°C, and mean maximum daytime

159 temperatures in June, July, and August of 6°C, 9°C, and 5°C, respectively. Mean annual precipitation is 79
160 mm. The number of ice-free days is variable and based on local climate conditions and elevation,
161 typically ranging from 40 days to 65+ days (Douglas and Smol, 1993). Eight of the 29 lakes and ponds
162 included in this study have been previously classified into “warm”, “cool”, and “cold” groupings, based
163 on local climate and ice cover regimes (Griffiths et al., 2017). Briefly, the two “warm” ponds (depth < 2
164 m), Col Pond and Elison Lake (Table 1), are located on Cape Herschel and have been repeatedly noted as
165 amongst the first in this region to lose their ice cover. A thermistor installed in Elison Lake recorded an
166 average of 92 ice-free days/year (from 2008-2010, determined as the number of days in one year
167 between pond temperatures rising above 0°C to when they first fall below 0°C; (M.S.V. Douglas, pers.
168 comm.). The “cool” sites, also located on Cape Herschel, include Moraine Pond, Paradise Pond and
169 Plateau Pond 2. These ponds are amongst the last in the region to lose their ice cover because they have
170 little shelter from the wind and occupy relatively high elevations or have other local features precluding
171 warming compared to the other sites (Griffiths et al., 2017). All the “cool” ponds had persistent
172 snowbanks in the catchment when sampled in 2011. The “cold” sites (Griffiths et al., 2017), located on
173 nearby Pim Island, are West Lake, Proteus Lake and Greely Pond. Although Greely Pond is shallow and
174 therefore melts completely during the summer months, historically West Lake and Proteus Lake have
175 typically maintained between 90 to 100% of their ice cover during the summer months, as observed
176 from field seasons dating back to the early 1980s. In 2011, however, the two lakes were largely ice-free
177 (Griffiths et al., 2017).
178
179 *Cajas National Park, Azuay Province, Ecuador* – The Andean study sites are in Cajas National Park
180 (2.83°S, 79.17°W) in southern Ecuador, near the city of Cuenca (Fig. 1). The Park is a páramo ecosystem
181 and contains over 800 lakes and ponds and covers 28,544 ha with elevations ranging from 3,100 to
182 4,450 m asl. The Park was established in 1996, in part, to protect the numerous lakes and waterbodies
183 that act as the main source of drinking water for the downstream city of Cuenca. There are no glaciers
184 within the Park and all waterbodies are fed primarily by precipitation. Seasonal variations in
185 temperature are minimal due to its equatorial location and diurnal temperature variations are greater
186 than that experienced annually. The nearby Cañar meteorological station (~30 km from the study sites)
187 shows a mean annual temperature (1960-2008) of 11.3°C. The seasonality of precipitation in the
188 Ecuadorian Andes is bimodal, with two main wet seasons from March to May and September until
189 November (Vuille, 2013). Annual precipitation ranges from 829 mm to 1,343 mm. Temperature data

from the Cañar meteorological station shows a warming trend since the early 1970s with an overall increase of 1.15°C since that time (Michelutti et al., 2015).

Nine lakes and ponds spanning elevations from 3,140 to 3,920 m were sampled in July 2011, August 2014, August to September 2015, and August 2016 (Table 1; Michelutti et al., 2015, 2016). Lake water samples in this study were collected at the end of the dry season (July to early September). Annual variations in daily solar radiation are minimal, and evapotranspiration is minimal (Michelutti et al., 2016). An air temperature data logger (HOBO Water Temperature Pro v2 Data Logger) was placed in a shaded area near the shore of the study site Laguna Toreadora (3,920 m asl) from August 2014 to September 2016 (ESM Table 1). Air temperatures were recorded hourly over this period, with an interruption in data collection from May to July 2015.

2.2 Sampling methodology and analysis

Water samples for stable isotope analysis were collected at ~10 cm depth from nearest the center of each site as possible in 30-ml high-density polyethylene bottles. The air-tight bottles were stored in a 4°C cold room at Queen's University until isotopic analysis was undertaken in 2015 and later in 2016 for some Ecuadorian sites. Isotopes were measured at the Ján Veizer (formally G.G. Hatch) Stable Isotope Lab at the University of Ottawa using the Los Gatos Research (LGR) Triple Water Isotope Analyzer with a measurement precision of ±0.8‰ for δ^2H and ±0.1‰ for $\delta^{18}O$. Results are reported in δ-notation relative to Vienna Standard Mean Ocean Water (VSMOW).

The GMWL ($\delta^2H = 8^* \delta^{18}O +10$; Craig, 1961) for precipitation is plotted in all δ^2H - $\delta^{18}O$ bivariate isotope plots to visualise the importance of snow-melt and summer precipitation to regional lake sets, as well as the degree of lake isotopic enrichment through evaporation. Local Meteoric Water Lines were determined by linear regression of δ^2H and $\delta^{18}O$ for Resolute Bay, the two locations nearest to Cape Herschel (Eureka and Alert) and Cuenca using data from the Global Network of Isotopes in Precipitation (GNIP; IAEA/WMO, 2021). Deuterium-excess (d-excess), calculated as d-excess = $\delta^2H - 8^* \delta^{18}O$ (Dansgaard, 1964) was determined for the Cape Herschel and Pim Island sites (ESM Table 2).

Climatological data from the three regions are discussed depending on their time resolution. Typically, at the Arctic sites, active snowmelt proceeds when air temperatures exceed 0°C and remain positive (Young and Abnizova, 2011), and thus we identified this day of year within each climate data set to help compare temperatures and approximate the potential starting day for the melting of lake ice

between sample years. The amount of precipitation from January 1st to July 31st was totaled in each Arctic sampling year to estimate the potential snowpack and spring snow melt occurring during or just prior to water collection. Using precipitation since January standardizes across all Arctic sites; however, precipitation as snow begins earlier than January in the Arctic, although there may be confounding factors (e.g., wind, sublimation) that could erode fall snowpack. Paired student t-tests were used to compare monthly mean daily temperatures between sampling years when complete data sets were collected.

3. Results

Water isotope characteristics for all study sites are given in Figs. 2-5 and summarized in Table 1 and in EMS Tables 2a, b, c. The Resolute LMWL is given by $\delta^2H = 7.8\delta^{18}O + 5.3$ ($n = 59$, $R^2 = 0.97$, $p<0.01$), which is close to the GMWL (Fig. 2). A much lower slope was generated for the LEL for all sites from 2009 to 2014, defined by $\delta^2H = 5.7\delta^{18}O + 43.5$ ($n = 27$, $R^2 = 0.98$, $p<0.01$). There was no overlap in δ^2H- $\delta^{18}O$ space in the study sites among the three sampling years (Fig. 2). The sites sampled in 2014 showed the least amount of evaporative enrichment and plotted closest to the LEL-LMWL intersection, which can be used to approximate the weighted mean isotopic composition of input waters (Edwards et al., 2004). In contrast, the 2011 sites showed the largest deviation from the LEL-LMWL intersection indicating the greatest amount of evaporative enrichment.

The Alert LMWL defined by $\delta^2H = 7.6\delta^{18}O + 1.6$ ($n = 59$, $R^2 = 0.99$, $p<0.01$) and the Eureka LMWL defined by $\delta^2H = 7.4\delta^{18}O – 9.1$ ($n = 55$, $R^2 = 0.97$) both lie close to the GMWL (Fig. 3a). The samples collected in 2009 and 2011 showed no clear separation from each other in δ^2H- $\delta^{18}O$ space, except for the 2011 samples from CH-Camp and CH-Beach Ridge (Fig. 3b). When examining the change in $\delta^{18}O$ from 2009 to 2011 in individual sites, 16 showed enrichment (with 3 sites recording a difference < 1‰) and 13 sites showed depletion (with 4 sites recording a difference <1‰; Fig. 4). Declines in d-excess values from 2009 to 2011 (Fig. 4) confirms enrichment over that period is due to evaporation.

The Cuenca LMWL (not shown) defined by $\delta^2H = 8.0\delta^{18}O + 10.2$ ($n = 24$, $R^2 = 0.99$) lies close to the GMWL (Fig. 5a). Except for the 2011 samples, there was overlap in sites among the sampling years in δ^2H- $\delta^{18}O$ space. Within each site, there was a progressive enrichment in $\delta^{18}O$ and δ^2H over time, however most values changed approximately parallel to the LMWL (Fig. 5b).

4. Discussion

4.1 Resolute Bay, Cornwallis Island

The Resolute Bay sites were the only study sites that showed no overlap among sampling years (2009, 2011, 2014) in δ^2H–$\delta^{18}O$ space (Fig. 2). Two hydrological processes that govern the isotopic composition of Arctic lakes and ponds (and have opposing effects) are snowmelt dilution and evaporative enrichment (Edwards et al., 2004). A useful metric to assess the timing of ice cover loss and by extension, evaporation, is the onset of the day in which temperatures remain persistently above 0°C. In 2011, the year with the most enriched water samples ($\delta^{18}O$ range: -14.4 to -7.3 ‰; Table 1), persistent temperatures above 0°C occurred on June 6. This is 26 days earlier than in 2014 (July 2), the year with water samples that showed the least amount of isotopic deviation from source water, approximated here by the intersection of the LEL with the LMWL ($\delta^{18}O$ = -22.1 ‰, δ^2H = -170 ‰; Fig. 2). Additionally, 2014 recorded exceptionally cold June air temperatures at Resolute Bay (mean temp: -1.31°C, normal: 0.4 ±1.5°C). In 2009, persistent temperatures above 0°C occurred on June 22, which is 16 days later than in 2011 and ten days earlier than in 2014. Accordingly, water samples from 2009 fell in between those of 2011 and 2014 in δ^2H–$\delta^{18}O$ space.

Precipitation varied among the study years and may also help explain the patterns recorded in the water isotopes. Total precipitation from January 1 to July 31 in 2011 was the lowest among study years at 58.4 mm, compared to 92.3 mm in 2009 and 83.3 mm in 2014 (Environment Canada, 2016). This low precipitation (and presumably less spring snowmelt compared to the other study years) in combination with earlier onset of above freezing temperatures may have contributed to 2011 samples showing the greatest enrichment (Fig. 2). The Resolute Bay data suggest that water isotopes sensitively track variability in climate variables among the study years. Rising evaporation to precipitation ratios with future climate change may lead to the eventual desiccation of these sites, as documented elsewhere in the High Arctic (Smol and Douglas, 2007b).

4.2 Cape Herschel and Pim Island, Ellesmere Island

Data from the Eureka meteorological station (nearest to Cape Herschel) show 2011 was warmer and drier than 2009. Although only three days separate the onset of persistent temperatures above 0°C (June 7 in 2009 and June 4 in 2011), mean temperatures for June and July in 2011 (5.6°C and 9.8°C, respectively) were notably warmer than in 2009 (4.0°C and 8.0°C, respectively). Total precipitation from January to July 31st was 34.4 mm in 2009 and slightly less at 27 mm in 2011.

At Cape Herschel, two ponds – Beach Ridge Pond (CH-BR) and Camp Pond (CH-Camp) – stand out as recording the greatest isotopic enrichment from 2009 to 2011 relative to all other sites (Fig. 3b). These ponds are among several from Cape Herschel that have undergone a documented "tipping point" beginning in the mid-2000s (Smol and Douglas, 2007b). Specifically, some ponds that have been permanent waterbodies for millennia, now occasionally completely desiccate beginning in July (Smol and Douglas, 2007b). Drainage via permafrost thaw, as has been described for some Siberian and Canadian sub-Arctic surface waters (Smith et al., 2005), is not the main cause of water loss at Cape Herschel, as these ponds are excavated in basins that are underlain by granitic bedrock. Rather, progressive increases in evaporation relative to precipitation due to warmer temperatures and extended ice-free conditions has been implicated as the most likely driver (Smol and Douglas, 2007b). This is supported by the meteorological data that show 2011 was generally warmer and drier than 2009. The small catchments of Beach Ridge and Camp ponds also likely make them more vulnerable to evaporation compared to other ponds at Cape Herschel.

Changes in the lake water isotopes between the study years appear to track climate-driven hydrological variability in some sites, especially in sites more prone to evaporation such as Beach Ridge and Camp ponds. Lower d-excess in lake waters generally indicate greater evaporation (Wen et al., 2016), and the low d-excess values indicate net evaporation from these sites (right-hand side of Fig. 4). However, unlike at Resolute Bay, not all study sites from Cape Herschel show enrichment in isotopic composition with warmer years (left-hand side of Fig. 4). Of the 29 Cape Herschel study sites, $\delta^{18}O$ shows an enrichment greater than 1‰ in 13 sites, less than 1‰ change in 7 sites, and a depletion greater than 1‰ in 9 sites. Thus, despite experiencing similar climatic conditions, the isotope data, including d-excess values, indicate substantial differences in water balance parameters (e.g., evaporation, meltwater input) among Cape Herschel sites (Fig. 4).

Some of the variation in isotopic composition is certainly related to site morphology. For example, the large lakes on Pim Island (i.e. P-West, P-260, P-Proteus), which traditionally retain summer ice cover, show either isotopic depletions or minimal enrichment (Fig. 4). Additional variability in isotopic composition between study years may be explained by the local topography at Cape Herschel, which, in comparison to Resolute Bay, is more variable (e.g. shaded and/or sheltered valleys) and has greater differences in elevation. This results in mesoclimates, which in turn affect the length of ice cover and may ultimately affect water balances as longer ice-free conditions allow for greater evaporation. Based on over 30 years of observational data, the study sites at Cape Herschel have been grouped into distinct microclimate categories. These include 1) "warm" sites that have long ice-free periods, 2) "cool"

318 sites that have shorter ice-free periods than the warm sites, and 3) “cold” sites that include waterbodies
319 that rarely lose their full ice cover (Griffiths et al., 2017). In this study, the “cool” (CH-Moraine, CH-
320 Paradise, CH-PP2) and “cold” (P-West, P-Proteus, P-Greely) sites show ^{18}O depletions (0.6 – 1.7 ‰)
321 between study years, except for P-Proteus, a cold site that shows a slight (<1‰) ^{18}O enrichment (Fig. 4).
322 The “warm” ponds (CH-Col and CH-Elison) have the longest ice-free periods and might be
323 predicted to show amongst the greatest amount of evaporative enrichment with warmer temperatures.
324 However, Elison Pond showed only a slight enrichment in ^{18}O (0.8 ‰) and Col Pond registered a
325 depletion (-2.6 ‰; Fig. 4). This suggests that these sites may be receiving a greater amount of
326 isotopically-depleted snowmelt. This is likely as Elison Lake is situated on a low-lying valley with
327 mountains on either side, with streams draining into the valley. One known example of meltwater
328 resulting in isotopic depletion (despite warming conditions) is in Pond 32, which recorded a small
329 depletion in $\delta^{18}O$ from 2009 to 2011 (-0.3 ‰; Fig. 4). Pond 32 was the only site that did not record an
330 increase in July conductance (an indicator of evaporative concentration of solutes) over a 24-year
331 monitoring period of warming temperatures (Smol and Douglas, 2007b). This pond occupies a low
332 position on the peninsula and receives snowmelt from several streams via the two high plateaus. Thus,
333 the meltwater this pond receives is borne out by its isotopic composition (Fig. 4, Table 1), which in turn
334 is supported by limnological data. Similarly, Bouchard et al. (2013) attributed a strong evaporative $\delta^{18}O$
335 enrichment response in sub-Arctic ponds to lower-than-average snowmelt runoff in recent years.
336
337 **4.3 Cajas National Park, Ecuador**
338 The study sites from Ecuador showed the most enriched isotopes of the three study regions with $\delta^{18}O$
339 ranging between -12.1 ‰ and -5.9 ‰ and $\delta^{2}H$ between -84.9 ‰ and -46 ‰ (Fig. 5), falling within values
340 measured elsewhere in Andean lakes (Abbott et al., 2003; Bird et al., 2011; Esquivel-Hernández et al.,
341 2018; Saylor et al., 2009). Hourly air temperature data collected at the study site Laguna Toreadora
342 showed that 2014 had, on average, significantly colder mean daily air temperatures from September to
343 December than in 2015 (monthly paired t-tests, $p<0.01$ for each month). The individual months of
344 January to April and July in 2016 were each significantly warmer than in 2015 (paired t-tests, $p<0.01$;
345 ESM Table 1). This follows the general warming trend recorded at the nearby (~30 km away) Cañar
346 meteorological station that showed a general warming trend of 0.29°C per decade since the early 1970s
347 (Michelutti et al., 2015).
348 The Andean lakes show δ-values that are offset from the LMWL, with most of the lakes plotting
349 below but approximately parallel to the LMWL over time indicating some influence from evaporation

(Fig 5b). The study lakes have no glacial input and are fed mainly by precipitation (Michelutti et al., 2015), although subsurface flow is also important in páramo ecosystems (Mosquera et al., 2016). Lakes within isolated catchments and with limited groundwater reserves and no fluvial input, will have their hydrologic mass balance dominated by precipitation (Bird et al., 2011). With high amounts of annual precipitation such as in Cajas National Park (range from 829 mm to 1,343 mm per year), water residence times are relatively short. This is supported by water residence times calculated for four of the Andean study sites including Larga (2.28 years), Toreadora (1.91 years), Patoquinas (0.5 years) and Llaviucu (0.11 years; Van Colen et al., 2017). Such short residence times are typical of tropical high elevation lakes, such as the Cajas National Park study sites, where the influence of evaporation on the lake's hydrologic and isotopic mass balance is minimal (Bird et al., 2011; Esquivel-Hernandez et al., 2018).

5. Conclusions

Our analyses reflect water balance parameters from three regions where dramatic limnological changes have been documented in recent decades (Douglas et al., 1994; Griffiths et al., 2017; Michelutti et al., 2015; Smol and Douglas, 2007a, b). The findings show that increasing air temperatures at Resolute Bay and Cape Herschel generally result in evaporative enrichment of water isotopes in the study ponds. However, several factors are important to consider when interpreting the isotope data including: (1) site morphology with deep, ice-covered lakes recording isotopic depletions or minimal enrichment compared to shallow ponds; and (2) topographic location where downstream sites receive greater amounts of isotopically depleted snowmelt compared to upstream sites. The Arctic data indicate that even small increases in air temperature, which lead to longer-ice free periods, can trigger evaporative water loss. Temperature-driven losses in water quantity underscore the important role that future trends in precipitation will play in maintaining and recharging these ecologically important ponds with continued warming. The Andean data indicate that temperature-driven evaporative water loss in the study lakes appears to be somewhat buffered by substantial precipitation from two wet seasons annually. Thus, although these lakes have experienced rapid physical and biological changes in recent decades due to rising temperatures (Michelutti et al., 2015), the isotope data indicate any enhanced evaporation has resulted in little change in water quantity. Overall waterbodies from High Arctic and tropical Andean locations are considered sentinels of climate change and the results from this study can serve as critical baseline data when assessing future impacts to aquatic ecosystems.

Acknowledgments

We thank Christopher Grooms, Dr. Andrew Labaj, Dr. Katie Griffiths, Dr. Emily Stewart, Rachel Melnik-Proud, Katherine McCleary, Dr. Marianne Douglas, and Dr. Kristopher Hadley for the collection of lake waters. This research was funded by a W. Garfield Weston Postdoctoral Fellowship to K.E. Hargan, the Natural Sciences and Engineering Research Council of Canada (NSERC), the Polar Continental Shelf Program (PCSP), and the Northern Supplement Training Program (NSTP).

Data Availability Statement

All data reported in this study are available at the Dryad digital repository. The air temperature data for Laguna Toreadora, Ecuador can be acquired at doi:10.5061/dryad.2ngf1vhqs. The stable isotope data for Eureka and Alert, Ellesmere Island can be acquired at doi:10.5061/dryad.fxpnvx0v0. The stable isotope data for Resolute Bay, Cornwallis Island can be acquired at doi:10.5061/dryad.4j0zpc8dq. The stable isotope data for Cajas National Park, Ecuador can be acquired at doi:10.5061/dryad.02v6wwq5h.

References

Abbott, M. B., Wolfe, B. B., Wolfe, A. P., Seltzer, G. O., Aravena, R., Mark, B. G., et al. (2003). Holocene paleohydrology and glacial history of the central Andes using multiproxy lake sediment studies. *Palaeogeography, Palaeoclimatology, Palaeoecology*, 194, 123–138. https://doi.org/10.1016/S0031-0182(03)00274-8.

Benjamin L, Knobel L. L., DeWayne Cecil L., & Green J. R. (2004). Development of a local meteoric water line for southeastern Idaho, Western Wyoming, and South-Central Montana. U.S. Geological Survey Scientific Investigations Report 2004-5126.

Bershaw J. (2018). Controls on deuterium excess across Asia. *Geosciences* 8, 257; doi:10.3390/geosciences8070257.

Bird, B. W., Abbott, M.B., Vuille, M., Rodbell, D. T., Stansell, N. D., & Rosenmeier, M. F. (2011). A 2,300-year-long annually resolved record of the South American summer monsoon from the Peruvian Andes. *Proceedings of the National Academy of Science*, 108, 8583–8588. https://doi.org/10.1073/pnas.1003719108.

Bouchard, F., Turner, K. W., MacDonald, L. A., Deakin, C., White, H., Farquharson, N., et al. (2013). Vulnerability of shallow subarctic lakes to evaporate and desiccate when snowmelt runoff is low. *Geophysical Research Letters*, 40, 6112–6117. https://doi.org/10.1002/2013GL058635.

Bowen, G. J., Cai, Z., Fiorella, R. P., & Putman, A. L. (2019). Isotopes in the water cycle: regional- to global-scale patterns and applications. *Annual Review of Earth and Planetary Sciences*, 47, 453–79.

Cluett, A. A., & Thomas, E. K. (2020). Resolving combined influences of inflow and evaporation on western Greenland lake water isotopes to inform paleoclimate inferences. *Journal of Paleolimnology*, 63, 251–268.

Craig, H. (1961). Isotopic variations in meteoric waters. *Science*, 133, 1702-1703.

Dansgaard, W. (1964). Stable isotopes in precipitation. *Tellus,* 16, 436-468.

Diaz, H. F., Bradley, R. S., & Ning, L. (2014). Climatic changes in mountain regions of the American Codillera and the tropics: historical change and future outlook. *Arctic, Antarctic, and Alpine Research*, 46, 735–743. https://doi.org/10.1657/1938-4246-46.4.735.

Douglas, M. S. V., & Smol, J. P. (1993). Freshwater diatoms from high arctic ponds (Cape Herschel, Ellesmere Island, NWT). *Nova Hedwigia*, 57(3-4), 511–552.

Douglas, M. S. V., Smol, J. P., & Blake Jr., W., (1994). Marked post-18th century environmental change in high-arctic ecosystems. *Science,* 266, 416–419.

Environment Canada (2016), Climate Data Online, http://climate.weatheroffice.gc.ca/climateData/canada_e.html (last accessed: 2016-06-01).

Edwards, T. W. D, Wolfe, B. B., Gibson J. J., & Hammarlund, D. (2004). Use of water isotope tracers in high-latitude hydrology and paleohydrology In R. Pienitz, M. S. V. Douglas, J. P Smol (Eds.), *Long-term Environmental Change in Arctic and Antarctic Lakes*. Kluwer Academic Publishers, Dordrecht, The Netherlands.

Esquivel-Hernández, G., Sánchez-Murillo, R., Quesada-Román, A., Mosquera, G.M., Birkel, C., & Boll, J. (2018). Insight into the stable isotopic composition of glacial lakes in a tropical alpine ecosystem: Chirripó, Costa Rica. *Hydrological Processes*, 32, 3588–3603.

Gibson J. J., & Reid R. (2014). Water balance along a chain of tundra lakes: A 20-year isotopic perspective. *Journal of Hydrology* 519 (Part B): 2148-2164.

Griffiths, K. T., Michelutti, N., Sugar, M., Douglas, M. S. V., & Smol, J. P. (2017). Ice-cover is the principal driver of ecological change in High Arctic lakes and ponds. *PLoS ONE*, 12(3), e0172989. https://doi.org/10.1371/journal.pone.0172989.

IAEA/WMO, 2021. Global Network of isotopes in precipitation. The GNIP database. https://nucleus.iaea.org/wiser

Labaj, A., Michelutti, N., & Smol, J. P. (2018). Cladocera in shallow lakes from the Ecuadorian Andes show little response to recent climate change. *Hydrobiologia*, 822, 203–216.

Larsen, J. N., Anisimov, O. A., Constable, A., Hollowed, A. B., Maynard, N., Prestrud, P., et al. Polar regions. In V. R. Barros, C. B. Field, D. J. Dokken, M. D. Mastrandrea, K. J. Mach, T. E. Bilir et al., (Eds.) Climate Change (2014). *Impacts, Adaptation, and Vulnerability Part B: Regional Aspects Contribution of Working Group II to the Fifth Assessment Report of the Intergovernmental Panel on Climate Change*. New York: Cambridge University Press; 2014. p. 71.

MacDonald, L. A., Turner, K. W., McDonald, I., Kay, M. L., Hall, R. I. & Wolfe, B. B. (2021). Isotopic evidence of increasing water abundance and lake hydrological change in Old Crow Flats, Yukon, Canada. *Environmental Research Letters* 16, 124024.

MacDonald L.A., Wolfe B. B., Turner, K. W., Anderson, L., Arp, C. D., et al. (2017). A synthesis of thermokarst lake water balance in high-latitude regions of North America from isotope tracers. *Arctic Science* (Special issue: Arctic permafrost systems) 3, 118-149.

Michelutti, N., Wolfe, A. P., Cooke, C. A., Hobbs, W. O., Vuille, M., & Smol, J. P. (2015). Climate change forces new ecological states in tropical Andean lakes. *PLoS ONE*, 10(2), e0115338. https://doi.org/10.1371/journal.pone.0115338.

Michelutti, N., Lemmen, J. L., Cooke, C. A., Hobbs, W. O., Wolfe, A. P., Kurek, J., & Smol, J. P. (2016). Assessing the effects of climate and volcanism on diatom and chironomid assemblages in an Andean lake near Quito, Ecuador. *Journal of Limnology*, 75, 275–286. https://doi.org/10.4081/jlimnol.2016.1451.

Mosquera G. M., Célleri R., Lazo P. X., Vaché K. B., Perakis S. S, & Crespo, P. (2016). Combined use of isotopic and hydrometric data to conceptualize ecohydrological processes in a high-elevation tropical ecosystem. *Hydrological Processes* 30, 2930–2947.

Roberts K. E., Lamoureux S. F., Kyser T. K., Muir D. C. G., Lafrenière M. J., Iqaluk, D., Pieńkowski A.J., & Normandeau, A. (2017). Climate and permafrost effects on the chemistry and ecosystems of High Arctic Lakes. *Scientific Reports* 7: 13292, DOI:10.1038/s41598-017-13658-9.

Rühland, K. M., Paterson, A. M., & Smol, J. P. (2015). Lake diatom responses to warming: reviewing the evidence. *Journal of Paleolimnology*, 54(1), 1–35. https://doi.org/10.1007/s10933-015-9837-3.

Saros J. E., Northington R. M., Osburn C. L., Burpee B. T., Anderson N. J. (2016). Thermal stratification in small arctic lakes of southwest Greenland affected by water transparency and epilimnetic temperatures. *Limnology & Oceanography,* 61, 1530–1542.

Saylor, J. E., Mora, A., Horton, B. K., & Nie, J. (2009). Controls on the isotopic composition of surface water and precipitation in the Northern Andes, Colombian Eastern Cordillera. *Geochimica et Cosmochimica Acta*, 73, 6999–7018. https://doi.org/10.1016/j.gca.2009.08.030.

Schindler D. W., Welch H. E., Kalff J., Brunskill G. J. & Kritsch, N. (1974). Physical and chemical limnology of Char Lake (75 °N lat). Journal of Fisheries and Resource Board of Canada, 31, 585–607.

Smith, L. C., Sheng, Y., MacDonald, G. M., & Hinzman, L. D. (2005). Disappearing Arctic lakes. *Science*, 308, 1429. https://doi.org/10.11 26/science.1108142.

Smol, J.P., Wolfe, A.P., Birks, H.J.B., Douglas, M.S.V., Jones, V.J., Korhola, A., Peinitz, R., Rühland, K.M., Sorvari, S., Antoniades, D., Brooks, S.J., Fallu, M.A., Hughes, M., Keatley, B.E., Laing, T.E., Michelutti, N., Nazarova, L., Nyman, M., Paterson, A.M., Perren, B., Quinlan, R., Rautio, M., Sauliner-Talbot, E., Siitoneni, S., Solovieva, N., Weckström, J., 2005. Climate-driven regime shifts in the biological communities of Arctic lakes. Proc. Natl. Acad. Sci. 102, 4397e4402.

Smol, J. P. & Douglas, M. S. V. (2007a). From controversy to consensus: making the case for recent climatic change in the Arctic using lake sediments. *Frontiers in Ecology and the Environment*, 5, 466-474.

Smol, J. P., & Douglas, M.S.V. (2007b). Crossing the final ecological threshold in high Arctic ponds. *Proceedings of the National Academy of Science USA*, 104, 12,395–12,397. https://doi.org/10.1073/pnas.0702777104

Stewart, E. M., McIver, R., Michelutti, N., Douglas, M.S.V., & Smol, J. P. (2014). Assessing the efficacy of chironomid and diatom assemblages in tracking eutrophication in High Arctic sewage ponds. *Hydrobiologia*, 721, 251–268. https://doi.org/10.1007/s10750-013-1667-6

Van Colen, W. R., Mosquera, P., Vanderstukken, M., Goiris, K., Carrasco, M.-C., Decaestecker, E., Alonso, M., Tamariz. F. L., & Muylaert, K. (2017). Limnology and trophic status of glacial lakes in the tropical Andes (Cajas National Park, Ecuador). *Freshwater Biology* 62, 458–473.

Vuille, M. (2013). Climate Change and Water Resources in the Tropical Andes. p. cm. (IDB Technical Note; 515).

Wen, R., Tian, L., Liu, F., & Qu, D. (2016). Lake water isotope variation linked with the in-lake water cycle of the alpine Bangong Co, arid western Tibetan Plateau. *Arctic, Antarctic, and Alpine Research*, 48(30), 563–580.

Woo M.-K. & Young K. L. 2003. Hydrogeomorphology of patchy wetlands in the High Arctic, polar desert environment. *Wetlands*, 23, 291–309.

Young, K. L., & Abnizova, A. (2011). Hydrologic thresholds of ponds in a polar desert wetland environment, Somerset Island, Nunavut, Canada. *Wetlands*, 31, 535–549. https://doi.org/10.1007/s13157-011-0172-9.

547 Table 1. Lake names, latitude and longitude, and $\delta^{18}O$ and $\delta^{2}H$ (‰VSMOW) for each study site.
548

			2009		2011		2014	
Resolute Bay (R)	Latitude	Longitude	$\delta^{18}O$	$\delta^{2}H$	$\delta^{18}O$	$\delta^{2}H$	$\delta^{18}O$	$\delta^{2}H$
R-10	74°42.428'N	94°59.771'W	-16.0	-131.7	-14.4	-123.9	-20.8	-163.5
R-11	74°42.513'N	94°59.623'W	-16.6	-133.9	-9.7	-100.1	-22.3	-173.1
R-12	74°42.532'N	94°59.424'W	-17.7	-139.0	-12.7	-117.0	-22.4	-173.9
R-13	74°42.604'N	94°59.391'W			-12.3	-115.8	-24.0	-173.0
R-2	74°42.837'N	95°00.704'W	-17.6	-145.5			-22.3	-169.5
R-4	74°42.809'N	95°03.524'W	-17.1	-144.1			-24.4	-182.3
R-5	74°42.661'N	95°03.593'W	-16.7	-140.1			-22.2	-176.6
R-C	74°42.160'N	94°53.385'W	-19.9	-156.5			-20.2	-160.1
R-M	74°41.872'N	94°58.893'W	-18.8	-149.4			-22.2	-166.2
R-R	74°41.500'N	94°57.255'W	-19.7	-157.3			-22.9	-181.4
R-Thule	74°40.550'N	94°55.255'W			-7.3	-84.9	-22.0	-166.9

			2009		2011	
Cape Herschel (CH) & Pim Island (P)	Latitude	Longitude	$\delta^{18}O$	$\delta^{2}H$	$\delta^{18}O$	$\delta^{2}H$
CH-Camp	78°37.010'N	74°40.711'W	-17.2	-139.8	-6.1	-81.5
CH-Elison	78°36.487'N	74°44.414'W	-15.0	-126.9	-14.2	-119.1
CH-EP	78°36.635'N	74°44.127'W	-16.0	-132.6	-14.2	-119.4
CH-HS	78°37.574'N	74°42.404'W	-12.7	-114.9	-11.6	-107.7
CH-Lagoon	78°36.288'N	74°44.364'W	-15.8	-131.4	-11.8	-112.7
CH-Paradise	78°36.530'N	74°46.117'W	-20.2	-154.3	-22.0	-165.4
CH-1	78°37.642'N	74°43.430'W	-15.8	-132.9	-14.0	-126.8
CH-7	78°37.519'N	74°42.808'W	-16.6	-131.6	-14.6	-132.5
CH-8	78°37.639'N	74°43.083'W	-16.8	-134.6	-12.0	-118.6
CH-10	78°37.641'N	74°43.241'W	-16.5	-135.7	-13.1	-119.3
CH-12	78°37.598'N	74°43.396'W	-15.7	-129.9	-17.1	-128.0
CH-13	78°37.619'N	74°43.522'W	-15.1	-129.2	-15.9	-122.7
CH-14	78°37.551'N	74°43.552'W	-16.2	-135.3	-16.1	-126.0
CH-15	78°37.464'N	74°41.037'W	-18.2	-144.6	-20.2	-158.5
CH-18	78°37.402'N	74°40.636'W	-17.9	-142.3	-13.4	-122.5
CH-28	78°37.434'N	74°43.717'W	-16.9	-134.1	-10.7	-101.8
CH-32	78°36.201'N	74°44.068'W	-22.0	-171.9	-22.2	-161.0
CH-PP1	78°35.832'N	74°38.769'W	-18.5	-146.0	-21.3	-156.5
CH-PP2	78°35.500'N	74°38.427'W	-20.3	-159.2	-21.6	-155.1
CH-PP3	78°35.366'N	74°36.109'W	-15.8	-140.4	-18.6	-142.4
CH-S7	78°37.497'N	74°42.907'W	-17.2	-137.3	-13.8	-128.2
CH-Beach Ridge	78°37.228'N	74°41.400'W	-15.3	-129.0	-2.2	-57.7
CH-Col	78°36.154'N	74°39.758'W	-18.7	-146.2	-21.2	-159.1
CH-W	78°37.229'N	74°42.419'W	-17.6	-140.1	-12.7	-121.8
CH-Moraine	78°36.685'N	74°40.977'W	-19.7	-155.8	-20.4	-156.3
P-Proteus	78°41.876'N	74°23.022'W	-19.7	-153.9	-18.9	-148.5

P-WEST	78°44.491'N	74°37.751'W	-19.0	-146.6	-20.4	-147.7		
P-GRE	78°44.379'N	74°16.201'W	-18.7	-148.8	-19.3	-154.2		
P-260	78°42.483'N	74°30.784'W	-20.0	-152.2	-21.9	-163.6		

			2011		2014		2015	
Cajas National Park	Latitude	Longitude	$\delta^{18}O$	$\delta^{2}H$	$\delta^{18}O$	$\delta^{2}H$	$\delta^{18}O$	$\delta^{2}H$
Apicocha	2°47.028'S	79°12.918'W			-7.8	-54.3	-6.3	-48.6
Toreadora	2°46.792'S	79°13.411'W	-11.2	-84.9	-10.8	-75.2	-9.4	-72.2
Patoquinas	2°46.910'S	79°12.523'W			-9.8	-70.6	-8.6	-66.3
Lado de Larga	2°47.565'S	79°14.739'W			-8.7	-65.6	-6.9	-56.2
Larga	2°47.601'S	79°14.695'W			-10.1	-74.5	-9.4	-71.4
Llaviacu	2°50.676'S	79°08.765'W	-12.1	-80.5	-10.5	-70.1	-9.5	-66.1
Negra	2°47.001'S	79°14.359'W	-11.0	-83.3	-8.0	-63.7	-7.2	-55.9
Fondocoha	2°45.677'S	79°14.182'W			-10.7	-76.1	-9.4	-70.2
Cajas	2°47.563'S	79°14.695'W			-7.2	-56.4	-6.0	-46.0

549

Figure 1. Location of the three study sites including: (1) Resolute Bay, Cornwallis Island, Nunavut, Canada; (2) Cape Herschel, Ellesmere Island, Nunavut, Canada; and (3) Cajas National Park, Ecuador. Map adapted from https://freevectormaps.com/globes/americas/GLB-AM-01-0001?ref=atr

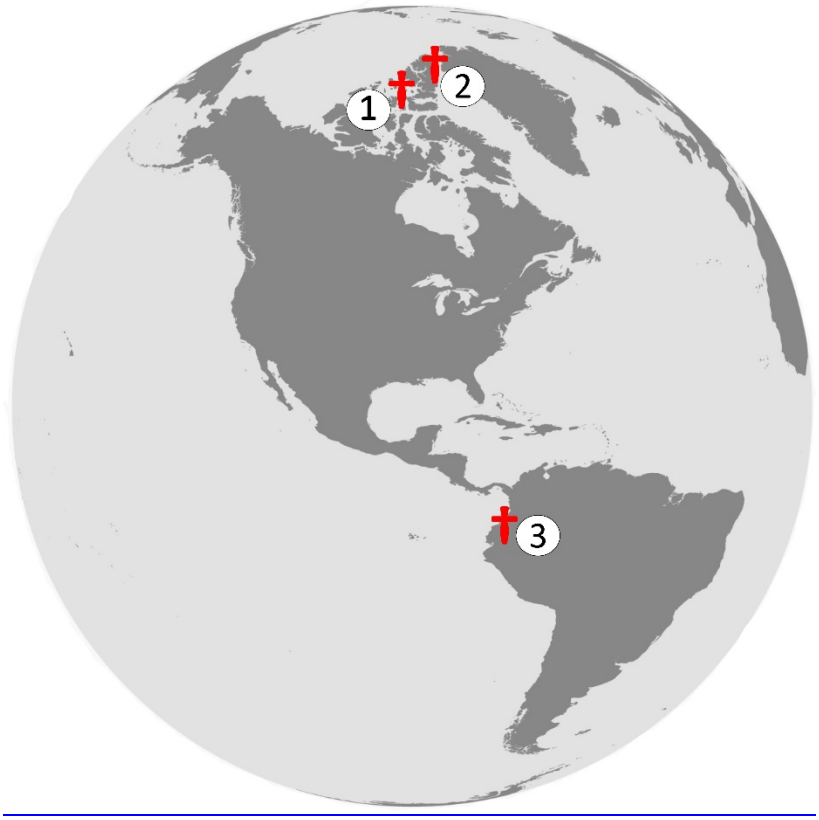

554 Figure 2. Graph of $\delta^{18}O$ versus $\delta^{2}H$ for Resolute Bay study sites sampled in 2009 (circles), 2011
555 (triangles), and 2014 (squares) plotted against the Global Meteoric Water Line (GMWL; solid black line),
556 the local meteoric water line for Resolute Bay (Resolute LMWL; dashed blue line), and the local
557 evaporation line (LEL; dotted red line) for all sites.

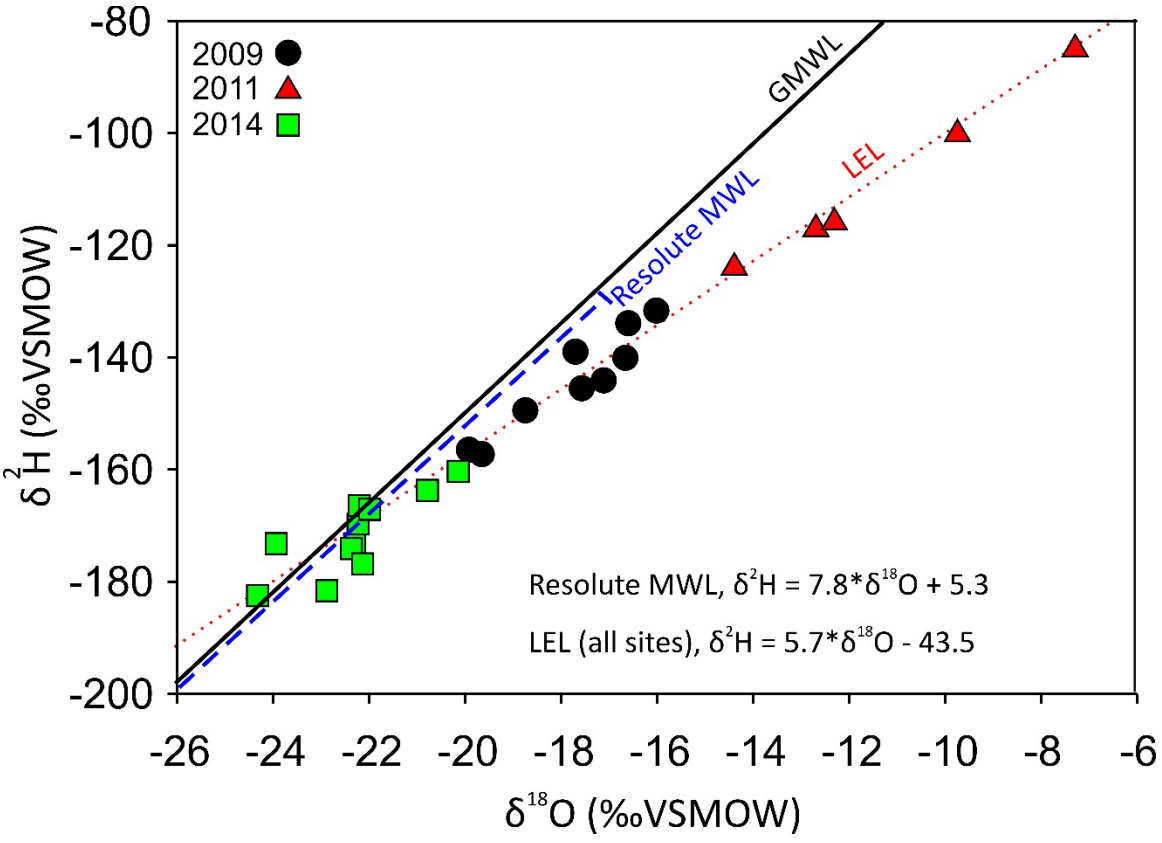

558

559 Figure 3. Graphs of $\delta^{18}O$ versus $\delta^{2}H$ showing (a) the Local Meteoric Water Lines for Alert (dotted blue
560 line) and Eureka (dashed green line), with the red square showing the region of interest in (b), which
561 shows the Cape Herschel study sites sampled in 2009 (circles) and 2011 (squares) plotted against the
562 Global Meteoric Water Line (GMWL; solid black line; GNIP; IAEA/WMO, 2021).

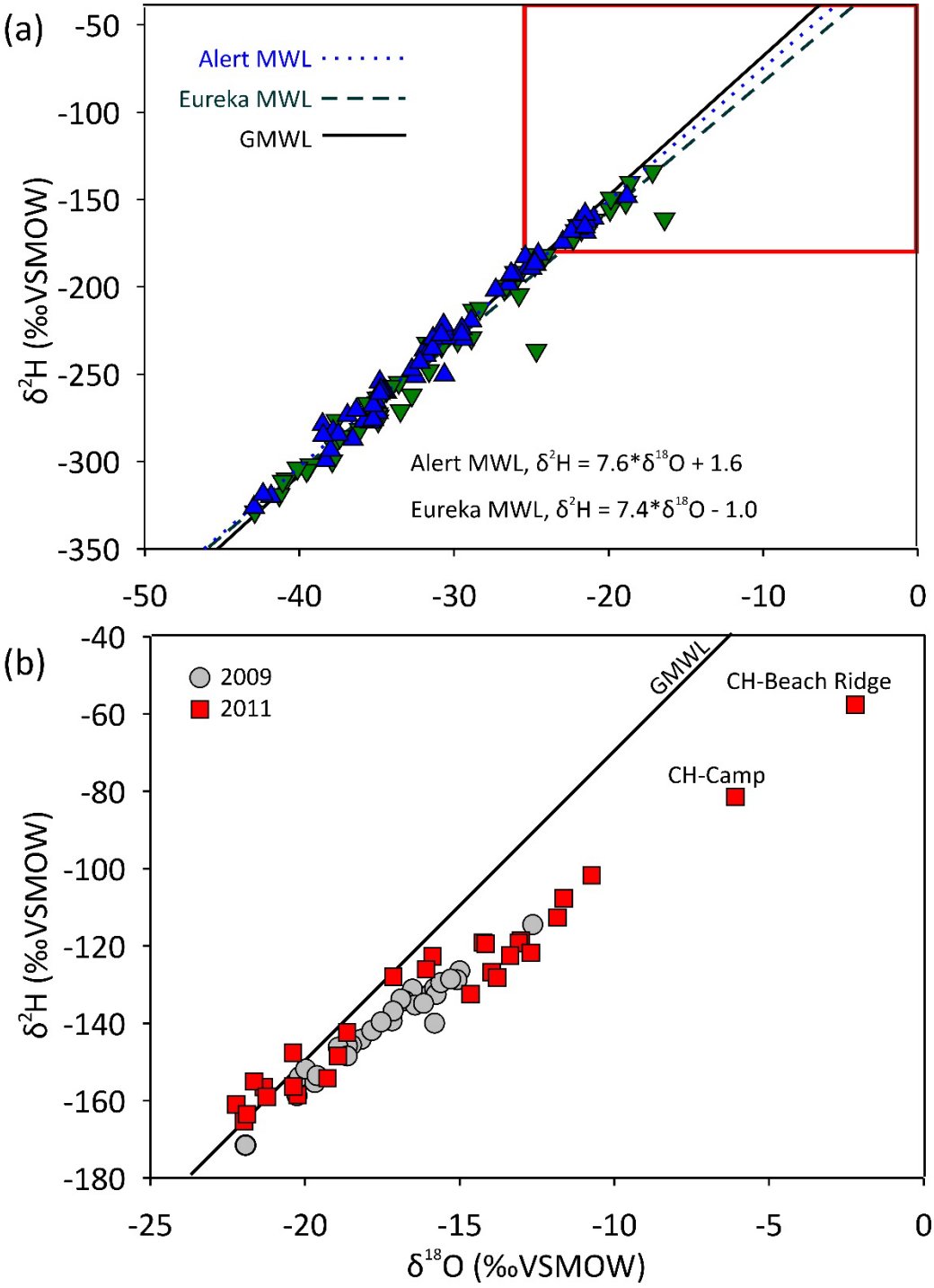

563

564 Figure 4. Graph showing the changes in the Cape Herschel study sites from 2009 to 2011 for (a) $\delta^{18}O$
565 (bars) and (b) d-excess (black and white circles).

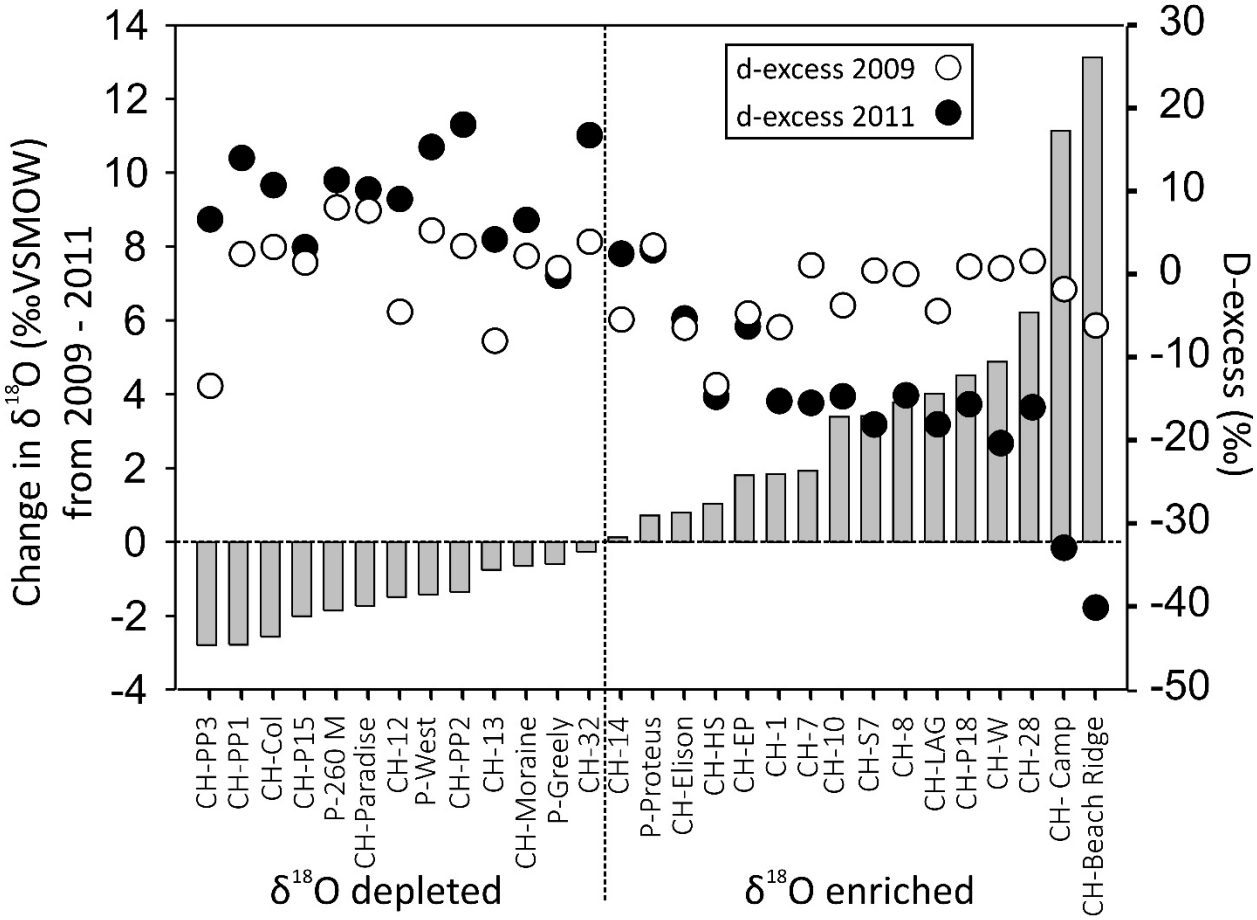

566

Figure 5. Graphs of $\delta^{18}O$ versus $\delta^{2}H$ showing (a) the Ecuador study sites sampled in 2011 (diamonds), 2014 (circles), 2015 (squares) and 2016 (triangles) plotted against the Global Meteoric Water Line (GMWL; solid black line) and the local evaporation line (LEL; dotted red line) for all sites and (b) the direction of change over time for each of the nine study sites.